Salt Gradient Solar Pond for Togolese Climatic Conditions

Magolmèèna Banna, Awourou Aregba, and Messan Gnininvi
Laboratoire Sur l'Energie Solaire
Université du Bénin BP 1515, Lomé
TOGO

ABSTRACT

An experimental pond has been installed and gradient generated. A thermal simulation program taking into account geoclimatic conditions is also prepared for analysing the performance of solar pond, and its optimal operation parameters. Preparation method of the density gradient in the salt water, correction procedure of the density gradient through appropriate technological tools, and analysis on the experimental results are described.

Effect of high wind velocity during harmattan, dust, and rainfall are observed on the thickness of upper convective zone and on the clarity of the pond brine.

The maximum temperature in the pond storage zone achieved was 86 °C, lower than the expected temperature. Reasons for not attaining higher temperature in the storage zone are discussed. However, the temperatures recorded although lower than the expected are sufficient for heating applications. A specific example is given for grain drying in the tropics.

1. INTRODUCTION

Solar ponds are inexpensive ways of collecting and storing solar energy. Small solar ponds can provide useful thermal output throughout the year. The developments in the world particularly in Israel and in USA [1, 2] have established its practical utility for power generation and have proved that solar ponds are quite appropriate for heating purpose. However, in tropical climates, very few demonstrations of technical and economical viability of small solar ponds have been achieved.

It is apparent that the pond efficiency depends on the atmospheric parameters. According to good climatic conditions that Togo benefits such as a high solar radiation, a high ambient temperature, high relative humidity, deep ground water table, and a small wind velocity, high performance of a solar pond in this region is expected.

In this present paper, an attempt is made to experiment and to asses the thermal performances and the viability of the solar pond under Togolese climatic conditions and to contribute to advance the basic knowledge of solar pond technology in the region. The work also focuses on applications that utilize the seasonal heat and storage capability of the solar pond for low-temperature thermal processes.

In order to set optimal operations parameters, a steady-state analysis of the salt gradient solar pond is carried out, taking into account both the surface and bottom heat losses. The performance of the steady-state solar pond is estimated for any given location with a knowledge of the geoclimatic

parameters like solar radiation, ambient temperature, relative humidity, wind velocity and water table depth. The effectiveness of the Upper Convective Zone (*UCZ*) as a heat sink is assessed for a given set of atmospheric parameters, as well as the optimal thickness of the Non Convective Zone (*NCZ*).

2. CLIMATIC CONDITIONS IN TOGO

The climate of Togo ranges from sub-equatorial with four seasons in the south, to tropical with two seasons and low rainfall in the north. Meteorological data indicates about 2660 hours annual sunshine in the north and 2090 hours in the south. The highest sunshine is experienced between October and April, with a daily average of 7.2 hours and total average solar radiation intensity of 4.5 kWh/m² per day at the ground. The least sunny months are June-September, which have a daily average of 5.5 hours and a solar intensity of 4.4 kWh/m² per day [3]. The relative humidity of the ambient air is very high, 90%-100% during the night and 50%-60% at noon in good weather. The estimation of monthly average hourly and daily global radiation on a horizontal surface have been carried out [4]. Figures 1 and 2 show the monthly variation of climatic parameters on the site of the pond (Lomé). The mean measured values of 10-years monthly average of the climatic parameters are shown in Table 1.

3. STEADY STATE ANALYSIS

3.1 Heat Losses from the Top Convective Zone

The effectiveness of the *UCZ* as a heat sink is assessed for a given set of atmospheric parameters. The heat losses from the surface (*UCZ*) of a solar pond due to radiation, convection and evaporation of the water at the surface are expressed as [5, 6]:

$$Q_s = \varepsilon_o \sigma (T_s^4 - T_{SKY}^4) + h_c (T_s - T_a) + [(L_T h_C) / (1.6\, C_s P_t)] (P_s - P_a) \quad (1)$$

Where the wind convective coefficient h_c is given by [7]:

$$h_c = 5.7 + 3.8\, V_a \quad (2)$$

Table 1. Solar and Climatic Data for Lomé

Climatic parameters in Lomé (6°11 N)	H_o (kWh/m²/day)	T_a (°C)	V_a (m/s)	ϕ (%)
Mean value	4.4	27	3	81

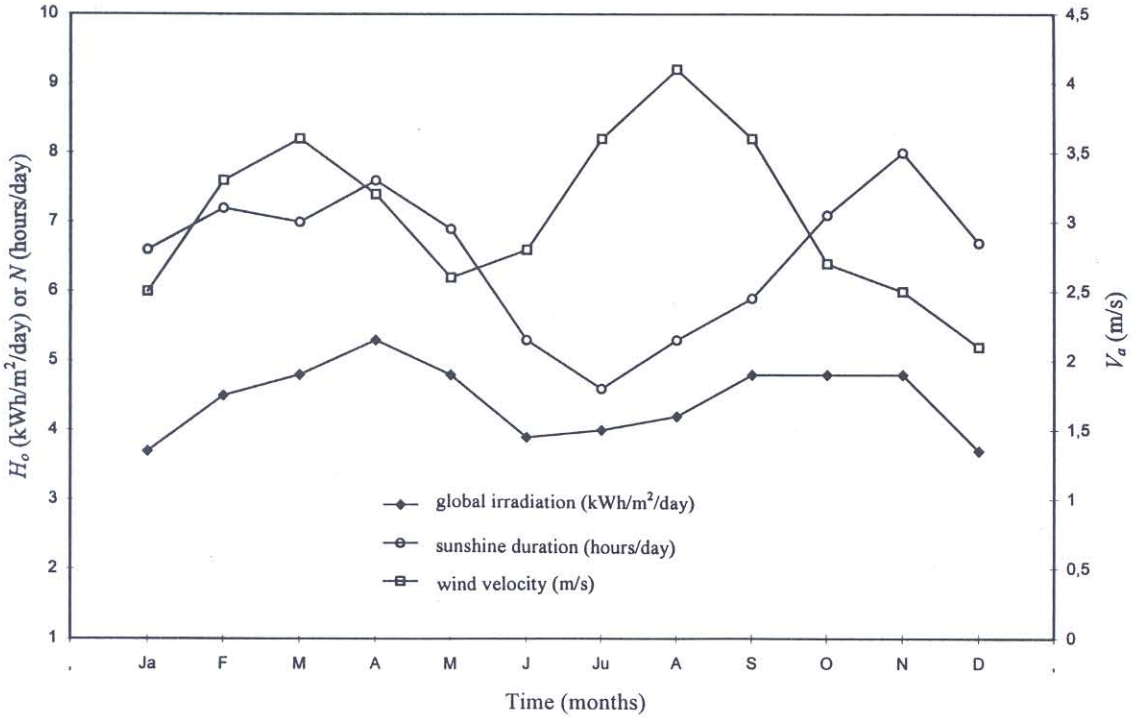

Fig. 1. Monthly variation of global irradiation, sunshine duration and wind velocity at Lomé.

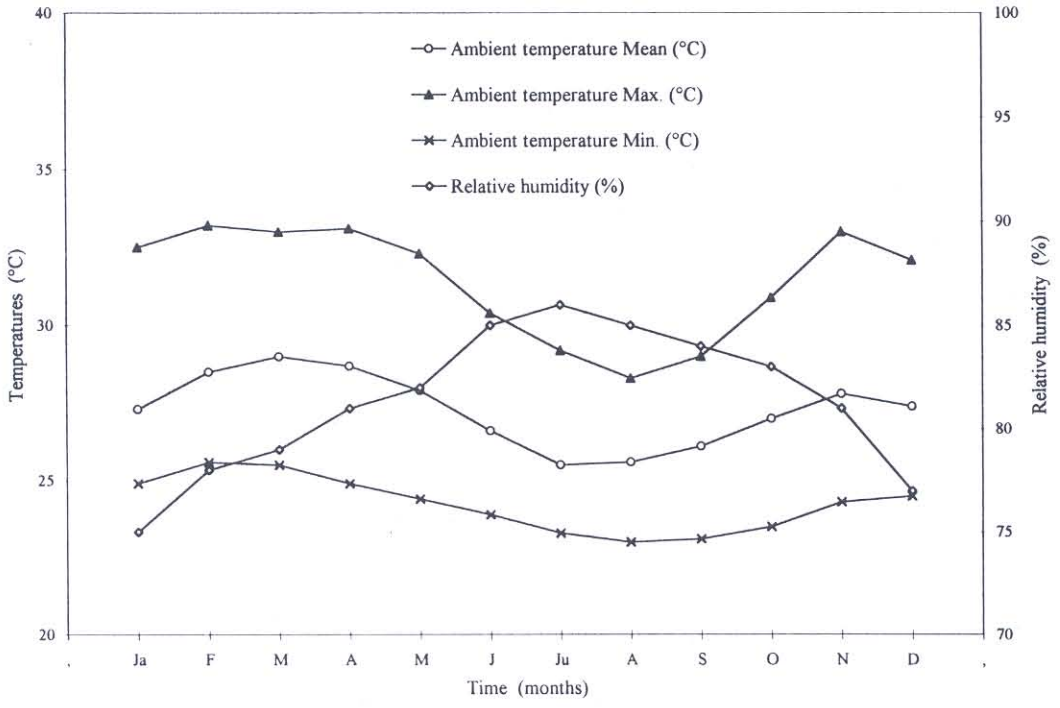

Fig. 2. Monthly variation af ambient temperature and relative humidity at Lomé.

The vapor pressure of water at the surface, P_s, is related to the surface temperature by the Antoine equation [8] given by:

$$P_s(T) = \exp(18.403 - 3885/(T_s - 43)) \quad (3)$$

By the definition of relative humidity, which is the ratio of the partial pressure of water vapor in the atmosphere, P_a, to the saturation vapor pressure of water corresponding to the ambient temperature, $P_s(T_a)$, the following equation is obtained:

$$P_a = \phi \exp(18.403 - 3885/(T_a - 43)) \quad (4)$$

The sky temperature T_{SKY}, can be expressed as [9] :

$$T_{SKY} = T_a (\beta [0.55 + 0.61 \sqrt{P_a}])^{0.25} \quad (5)$$

$$\beta = 1 + 0.224N - 0.0035N^2 + 0.0028N^3 \quad (6)$$

where N is the cloud cover.

3.2 Heat Losses from the Bottom Convective Zone

The ground losses is evaluated using an empirical equation [10]:

$$Q_b = U_b (T_b - T_g) \quad (7)$$

where U_b is a bottom heat loss coefficient given by:

$$U_b = 0.99 (K_g/L_g) + 0.9 K_g (P_e/A_c) \quad (8)$$

3.3 Steady-State Model for the Pond

The one-dimensional steady heat conduction equation governing the non-convecting zone is written as:

$$K (d^2T/dx^2) = H_o (1 - \varepsilon)(dg/dx) \quad (9)$$

where ε is the albedo of the surface, and depends on incidence angle of the solar radiation. The attenuation function $g(x)$ depends mainly on the transparency of the water used in the pond and many expressions are available [11, 12] to evaluate $g(x)$.

The solution of Eq. 9 requires two boundary conditions, which can be attained by making energy balance on the *UCZ* and *LCZ*. The energy balance for the *LCZ* can be written as:

$$H_o (1 - \varepsilon)\, g(x_2) - K [dT/dx]_{x=x_2} - Q_b - Q_u = 0 \quad (10)$$

where Q_b is the heat loss from the *LCZ* and Q_u is the useful heat extraction rate. An energy balance for the *UCZ* can then be written as:

$$Q_s = H_o (1 - \varepsilon) [1 - g(x_1)] K [dT/dx]_{x=x_2} \quad (11)$$

Integrating Eq. 9 once, the following equation is obtained:

$$K [dT/dx] = H_o (1 - \varepsilon) g(x) + C_o \quad (12)$$

where C_0 is an integration constant. With the upper boundary condition given by Eq. 11, the integration constant C_0 is obtained as:

$$C_0 = Q_s - H_o (1 - \varepsilon) \quad (13)$$

Substituting the value of C_0 from Eq. 13 in Eq. 12 and integrating between the limits x_1 and x_2, the following equation is obtained:

$$Q_s = H_o (1 - \varepsilon)(1 - \alpha\tau) - U_L (T_b - T_S) \quad (14)$$

Following Kooi [11], a transmittance-absorptance product $\alpha\tau$ and a top loss coefficient U_L are defined as:

$$(\alpha\tau) = \int_{x_1}^{x_2} g(x)\, dx/(x_2 - x_1)\ ;\ U_L = K/(x_2 - x_1) \quad (15)$$

From Eq. 1 and Eq. 11, the equation connecting the *UCZ* temperature T_S to both pond parameters and atmospheric parameters is obtained as:

$$H_o (1 - \varepsilon)(1 - \alpha\tau) - U_L (T_b - T_S) = \varepsilon_o \sigma (T_S^4 - T_S^4) + h_c (T_s - T_a) + 2.2\ (P_s - P_a) \quad (16)$$

For a given set of operational conditions, the parameters $\alpha\tau$, U_L, T_b, and Q_b are fixed in which case Eq. 16 can be solved to find the value of T_S for given atmospheric parameters. The value of T_S so obtained can be compared with the design sink temperature.

The useful heat to be extracted can be obtained from Eq. 10 in conjunction with Eq. 12 and Eq. 13 and can be written as:

$$Q_u = \alpha\tau (1 - \varepsilon) H_o - U_L (T_b - T_S) - Q_b \quad (17)$$

With a knowledge of the daily average values of H_o, ε, ϕ and V_a, etc. and for a given location (as characterized by K_g, L_g, and T_g), the efficiency of the pond for a given or desired value of T_b can be estimated from the equation below:

$$\eta = (1 - \varepsilon)\, \alpha\tau - U_L\ (T_b - T_S)/H_o - U_b (T_b - T_g)/H_o \quad (18)$$

3.4 Optimization of Gradient Zone Thickness

If gradient zone is thin, the heat loss by conduction transfer will be large and the efficiency low; if it is very thick the amount of light reaching the *LCZ* will be small and the efficiency will again be low. Between these extremes there is a thickness of the *NCZ* ($\Delta x = x_M - x_1$) which will maximize the efficiency. It is found by setting $d\eta/dx_2 = 0$ and $x_2 = x_M$.

$$x_M + x_1 [L_n(x_1) - L_n(x_M) - 1] = K [\Delta T / (1 - \varepsilon) b H_o] \quad (19)$$

The temperatures of the *UCZ* and the *LCZ* and the value of the solar radiation have been fixed so that ΔT constant.

4. EXPERIMENTAL FACILITY

The work was centered around 200 m² cylindrical salt-gradient solar pond experimented at the laboratory in Lomé (Fig. 3). The pond is 16 m in diameter, 4 m in depth and contains about 740 m³ of water (3.7 m in depth) and 130 000 kg of sodium chloride salt (about 18% of salinity). The pond was constructed in reinforced concrete and insulated with a 200 mm kapok layer. The pond was covered with a back plastic liner made-to-measure by Seaman Corporation (U.S.A.) in order to prevent leakage of the salt water into the surrounding ground and to increase the solar absorption efficiency.

One of the aims of this work was to asses the technical and thermal efficiency of small solar ponds in Togo, for process heat and power generation. A net work of 39 underground thermocouples (E-type) connected to a data acquisition system was used to measure the soil temperature distribution below the pond and to appreciate the heat losses (Fig. 4). A vertical moving thermocouple measures the temperature profiles within the pond. Two diffusers made by two circular plexiglas plates, fixed on PVC tubes and joined to a pump were set up at the top of *LCZ* for the establishment and the correction of the salt gradient in the pond.

4.1 Salt Gradient Establishment and Maintenance Procedures

The solar pond salt gradient serves as a transparent layer of insulation. It is imperative that this salt gradient be established and maintained properly. The pond was filled initially with fresh water up to the appropriate depth [13] of the gradient zone. All the salt was then dissolved in the water and the solution mixed to make a homogeneous brine. Fresh water was then floated onto the surface of the brine so that the pond was filled to the full operational level. This fresh water was subsequently pumped from the surface of the pond into a brine diffuser and injected into the high density brine solution.

Gradient maintenance is essential to the long term operation of the pond. It is important to monitor the salt gradient zone densities and to correct any instabilities that may occur within the salt gradient zone because the destablishment of the gradient zone affects consequently the pond efficiency. For this reason, regular gradient correction was carried out. Density within the pond was measured using a weighing method in order to monitor the brine salinity.

5. RESULTS AND OBSERVATIONS

5.1 Steady-State Model

Many workers assumed that surface temperature T_s is equal to the ambient temperature T_a, and Kooi has taken T_s as equal to the average wet bulb temperature T_w. The values of η calculated by Kooi's equation both for $T_s = T_a$ and $T_s = T_w$ are shown in Fig. 5 for different values of bottom temperature T_b, along with the values calculated by Eq. 16.

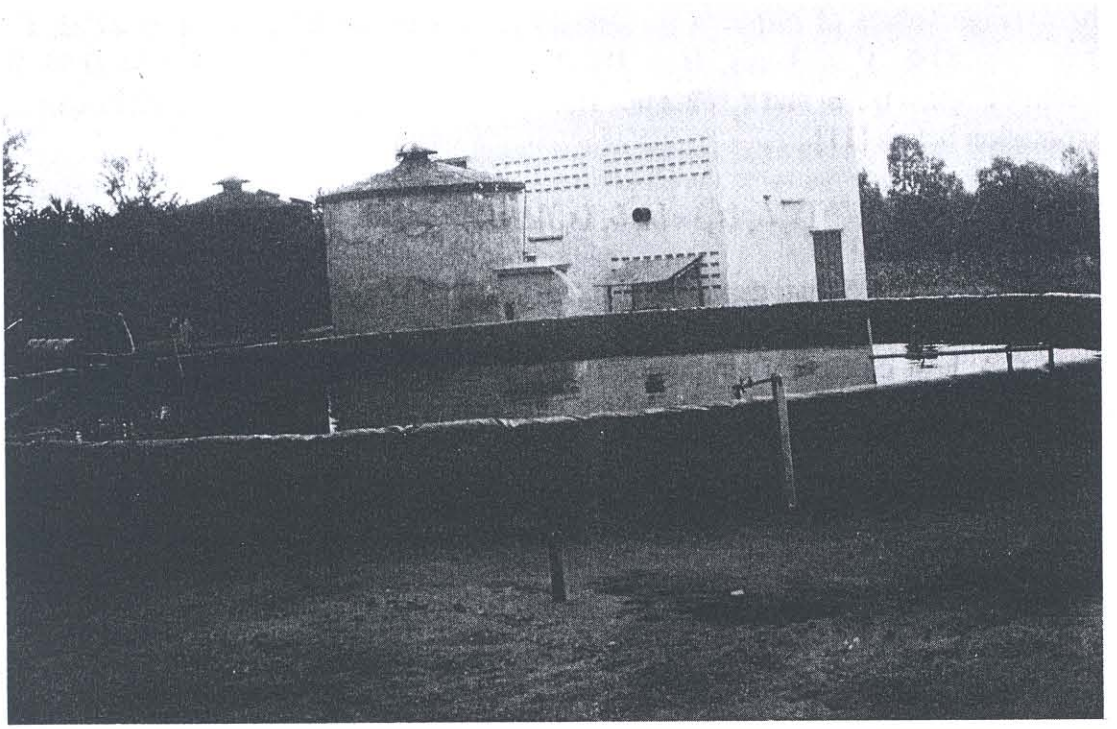

Fig. 3. General view of the solar pond area.

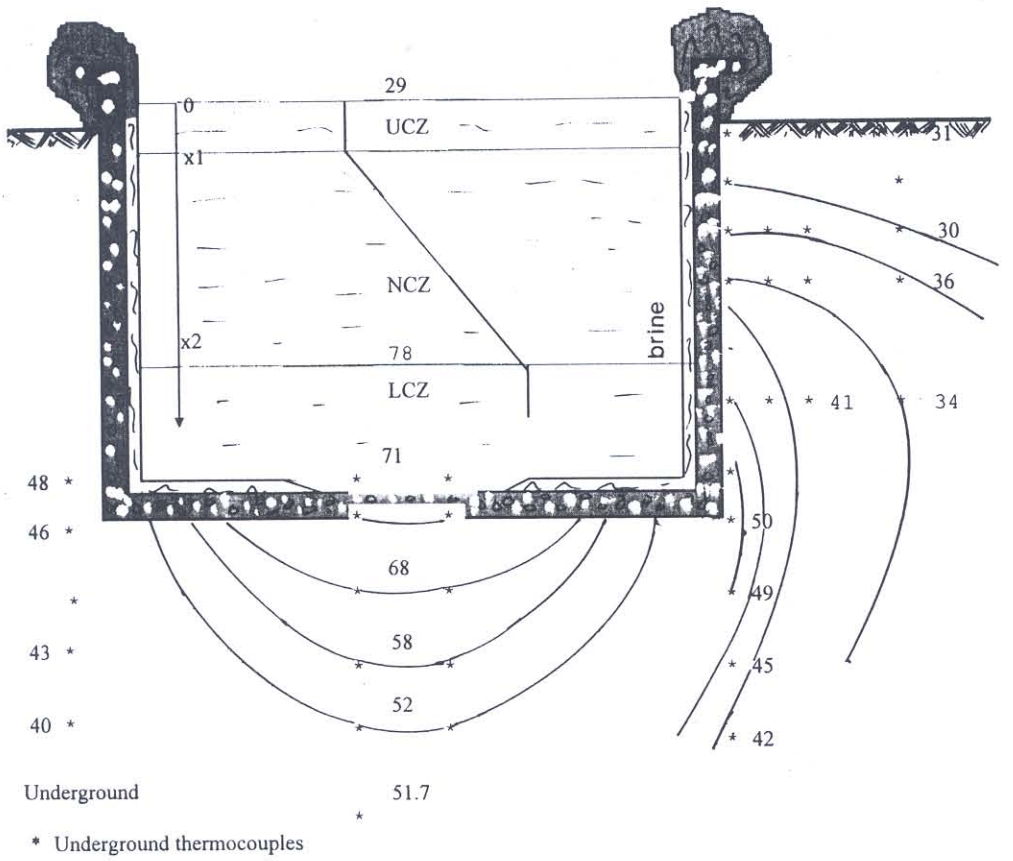

Fig. 4. Schematic diagram of the pond and temperature distribution in the ground.

The average values of different parameters chosen are as follows: T_a = 27°C, T_g = 30°C, L_g = 20 m, ϕ = 81%, V_a = 3 m/s, H_0 = 186 Wm^{-2}, ε = 0, A_C = 200 m^2, K = 0.64 $Wm^{-1}°C^{-1}$, K_g = 1.5 $Wm^{-1}°C^{-1}$, x_1 = 0.2 m and x_2 = 2.2 m. The transmittance-absorptance product was calculated by the expression below [11].

$$\alpha\tau = a + b - b\,[x_2 L_n(x_2) - [x_1 L_n(x_1)]/(x_2 - x_1) \text{ with } a = 0.36, b = 0.08 \quad (20)$$

It is clear from Fig. 5 that, depending on the geoclimatic conditions, the thermal efficiency of solar pond deviates substantially from that predicted by Kooi's equation. For a given average surface temperature (T_s), heat collection temperature (T_b), and solar irradiation (H_0), there is an optimal thickness of the nonconvective zone for which the heat collection efficiency is a maximum. The optimum gradient thickness (Δx) condition (Eq. 16) is graphed in Fig. 6 with the thickness of the *UCZ*, x_1, as a parameter. This set of curves is used to determine the average optimum x_2 value obtainable for a given x_1 and T_b. For an expecting temperature T_b = 95°C, and for a temperature T_s calculated with the average climatic parameters (Table 1), it is found from Fig. 5 an efficiency of 11% for x_1 = 0.2 m. Under these conditions, the optimum value of gradient thickness Δx calculated by Eq. (19) is 2.08 m. These parameters have been chosen and used to establish and to correct the salt gradient within the pond.

5.2 Experimental Results

Brine Clarity and Density History

Pond clarity is one of several factors which determines the temperature increment attainable, and controls the fraction of incident energy extractable for a given temperature increment. As clarity substantially effects the economics of pond use for a particular application, priority must be given to establishing a clean pond and thereafter its maintenance. Golding and Nielsen [14] gave a review of turbidity in solar ponds (organic color, micro-organisms...) and presented different artificial and natural clarification techniques particularly tested in Australia. The phenomena responsible for the clarity disturbance described by Golding and Nielsen are nearly the same under Togolese climatic conditions. Indeed, during high windy periods at Lomé (harmattan), lot of dust gets blown over the pond and algal growth is also observed. In the initial period it remains suspended in the *UCZ* and after agglomeration settle down. Addition of alum (generally used to clear water in Togo) and copper sulphate as algaecide is regularly practised to take care of above problems.

The monitoring of the pond behavior indicates that the performance was correlated with the geoclimatic parameters. The density profiles in the three zones of the pond are shown in Fig. 7. The variation sharply contrasts with the profiles reported for several solar ponds and indicates that the method used to establish the gradient is satisfactory. NaCl solution in the *LCZ* was maintained at saturation with piles of undissolved salt; that explains the salinity profile discontinuity on 300 mm near the bottom of the pond. The development of salt concentration profile are similar to those studied by Akbarzadeh and Ahmadi [15] in the case of various surface and bottom salt concentration and different values for salt diffisivity in the pond.

The position of the boundary between the gradient zone and the upper convective zone varies somewhat through the year. It moves downward as the pond temperature increases, due to the increasing temperature gradient at the top of the gradient zone (Fig. 8). The upper boundary instability was created mainly by the water evaporation and salt diffusion. The upper thickness since set up at 0.2 m moved down slowly and reached 0.7 m during the harmattan when wind velocity is high

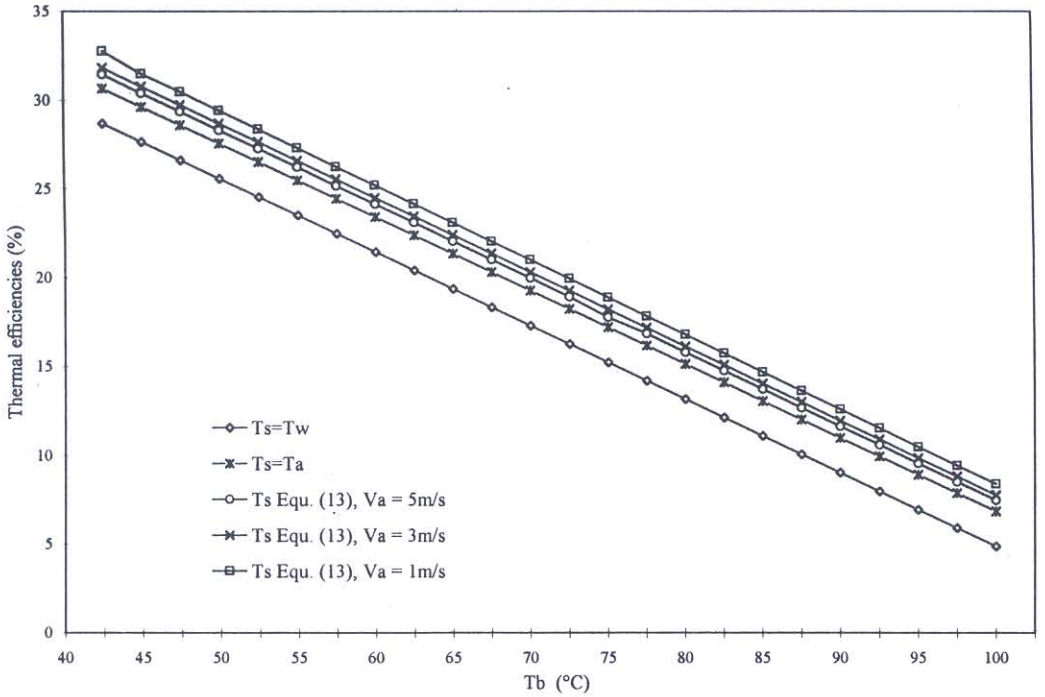

Fig. 5. Comparison of thermal efficiencies of the solar pond obtained in the the present work (Eq. 16) with those obtained by Kooi's equation.

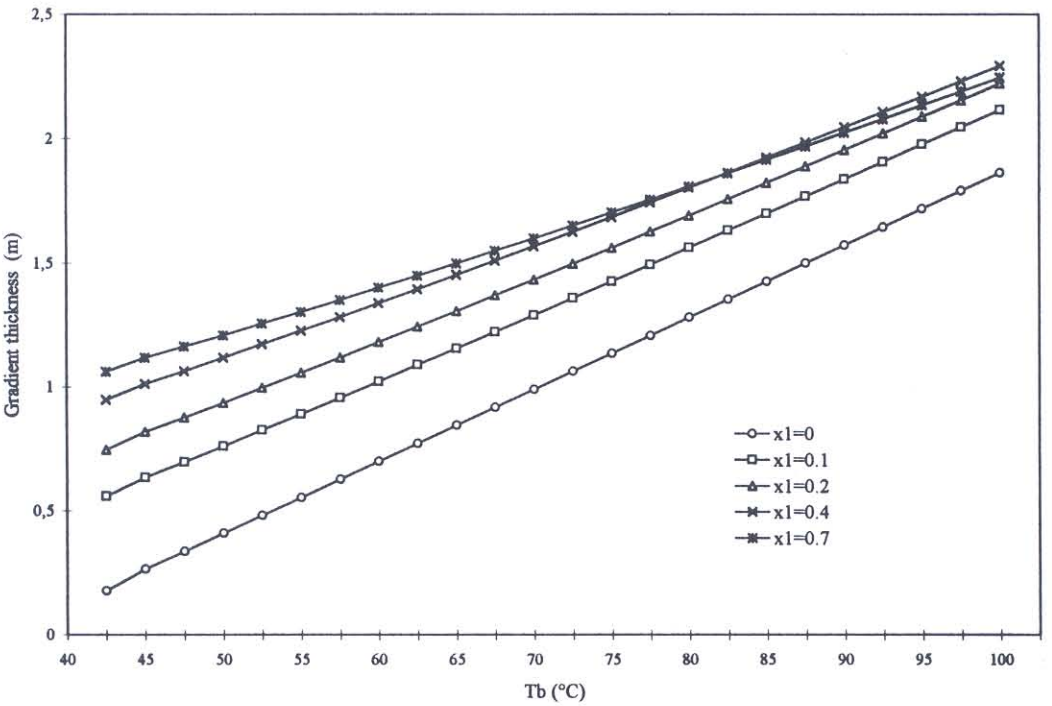

Fig. 6. Graph of the thickness of the *LCZ*, when $x_2 = x_4$ for the maximum efficiency, as a function of T_b.

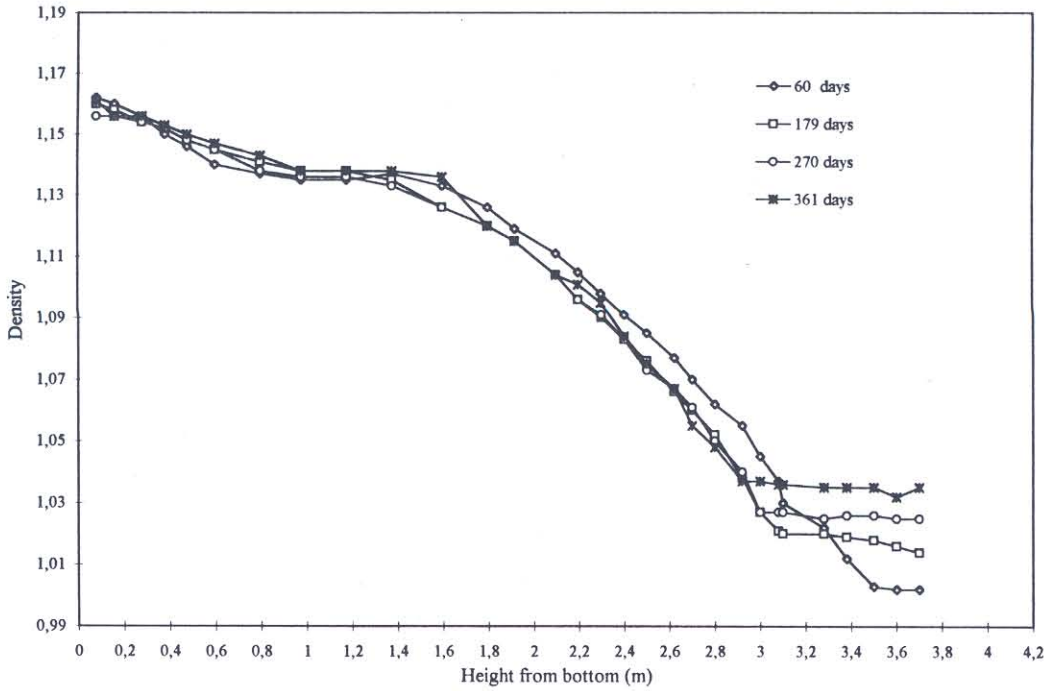

Fig. 7. Variation of brine density with depth in a salt solar pond.

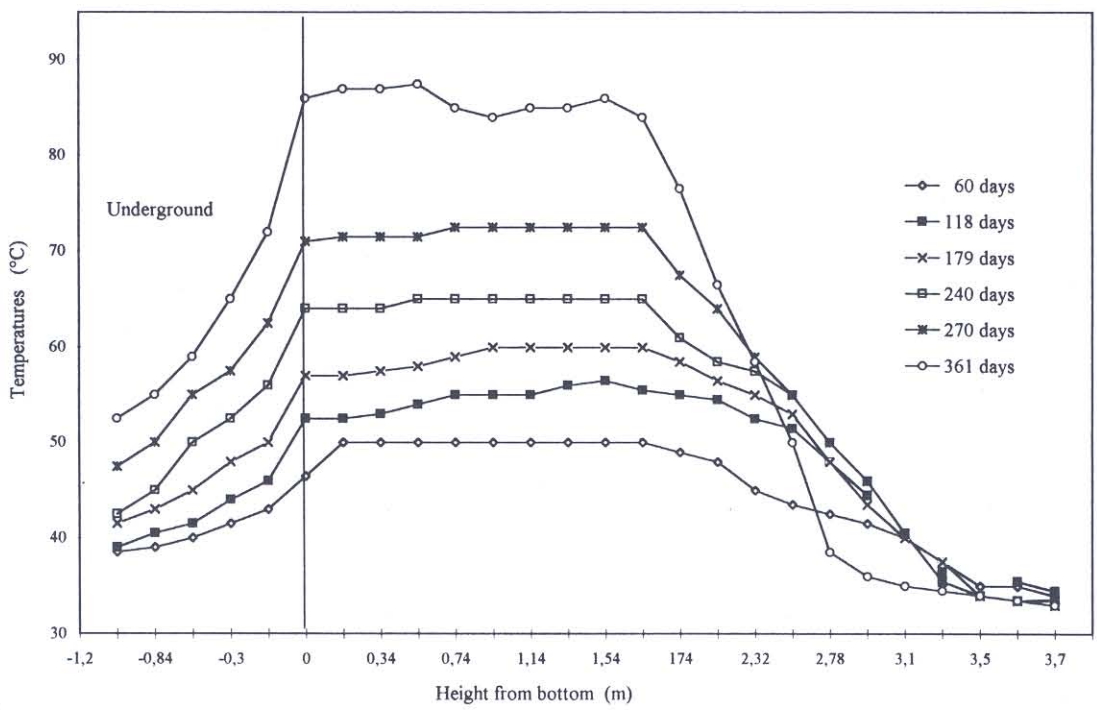

Fig. 8. Variation of brine temperature with depth in a salt solar pond.

(Fig. 7). Salt slowly diffuses upwards through the solar pond gradient at variable rate. The rate was high during the harmattan and reached a monthly average rate of about 200 g/cm². During this diffusion process, the surface zone slowly becomes more salty and the storage zone loses some of its salt.

Gradient Maintenance

Several tests permitted to draw out a method for gradient maintenance through appropriate technological tools. To re-establish solar pond, some of the surface zone brine were often disposed of, replaced with fresh water, and new salt added to the storage zone of the pond. This was done simply by pumping away the surface brine into a brine diffuser to the injection diffuser set in the *NCZ*, dispose of it in acceptable manner, and introduce salt to the bottom of the pond to replace the salt that has been discarded. Fresh water is then introduced onto the surface of the pond in order to re-establish the pond surface level. The process was repeated with successively decreased proportions of fresh water at *UZC* to give layer of increasing salinity until the desired nonconvective layer and upper layer were reached at their optimal positions. Figure 9 shows the density profiles before and after the gradient correction. The first corrections have been carried out each 3 months since the initial operation of the pond. Heat extraction has reduced the gradient disturbance and the next correction has been carried out 5 months after.

Temperature History

Since the initial operation of the solar pond, the pond has continued to successfully accumulate and store heat, gradually warning the ground underneath the pond. No heat was extracted during the first year of the pond operation. The temperature history within and in underground of the pond are shown in Fig. 8 and Fig. 10. The temperature of the storage zone of the pond increased rapidly and attained a maximum value of 86°C after one year. After the pond achieved its maximum temperature, the temperature difference between the top and bottom of the pond remained almost constant for a period of 5 months. The position of the boundary between the gradient zone and the *LCZ* has been fixed during the operational history of the solar pond. The reason for the stability of this lower boundary is the presence of the large salt piles at the bottom of the pond. The physical phenomena causing the boundary stability are similar to those used by Akbarzadeh and MacDonald [16] in stabilizing their solar pond. However, rather than external tanks and pipes, only a salt pile is needed in the pond experimented at Lomé.

It was expected that this pond will achieved a temperature above 95°C in the *LCZ*, but the data show that the expected results have not been achieved. The upward conduction losses from *LCZ* to *UCZ* and the ground heat losses although lower appear to be playing important role. Calculated optimum thickness of *NCZ* less than the observed thickness is one of the reasons for large conduction heat loss from *LCZ* to *UCZ*. The dirty and undissolved salt accumulating at the bottom of the pond can reduce its ability to absorb solar radiation. Guha [17] has shown that the reflectivity of salt to solar radiation is between 0.4 to 0.6 and 0.1 for dirt. The undissolved salt at the bottom although playing an important role in stabilizing the pond, has reduced the pond thermal performance.

Figures 11 and 12 show respectively the effect of the rainfall on temperature history and on brine depth in the pond. Temperatures recorded before and after the rainfall of 20 mm or 30 mm indicated the falling temperature about 2.0°C in the pond.

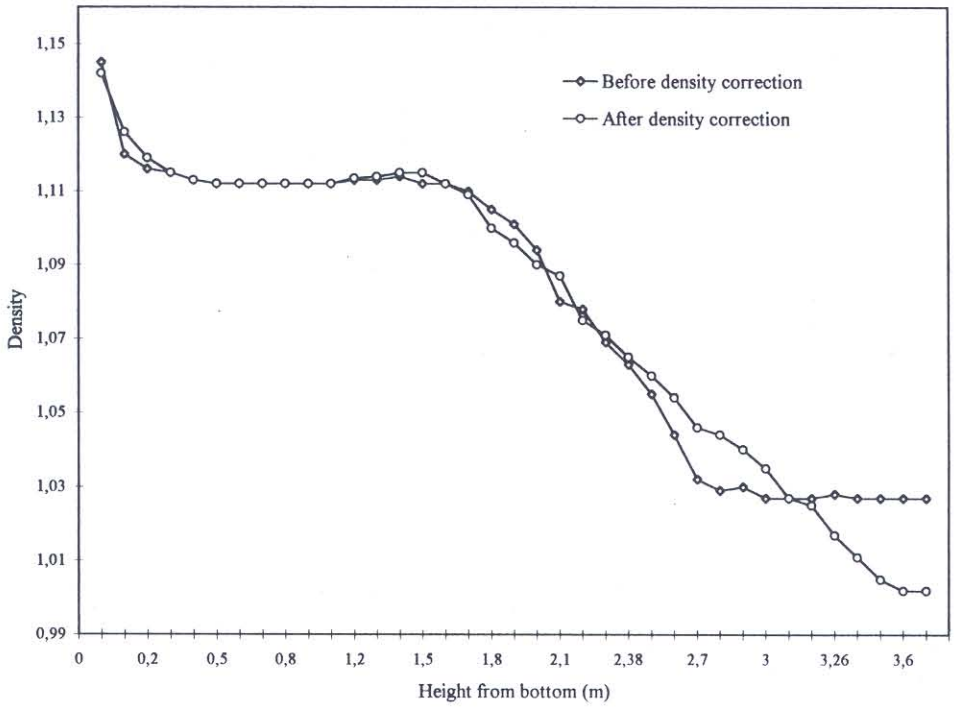

Fig. 9. Density profiles before and after the gradient correction.

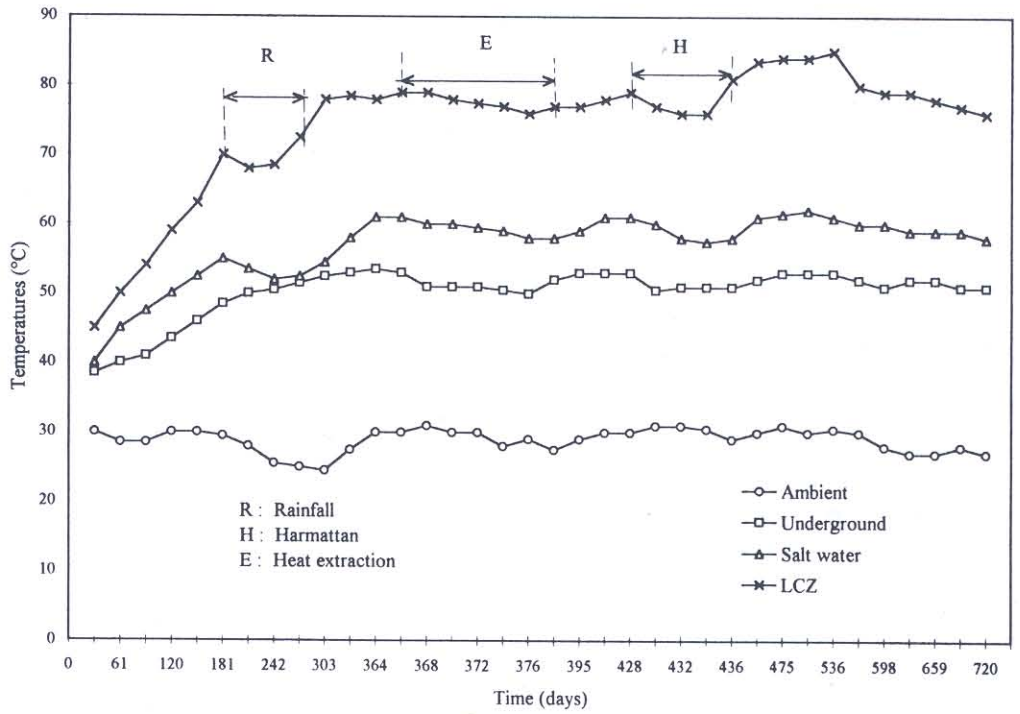

Fig. 10. Temperature profiles.

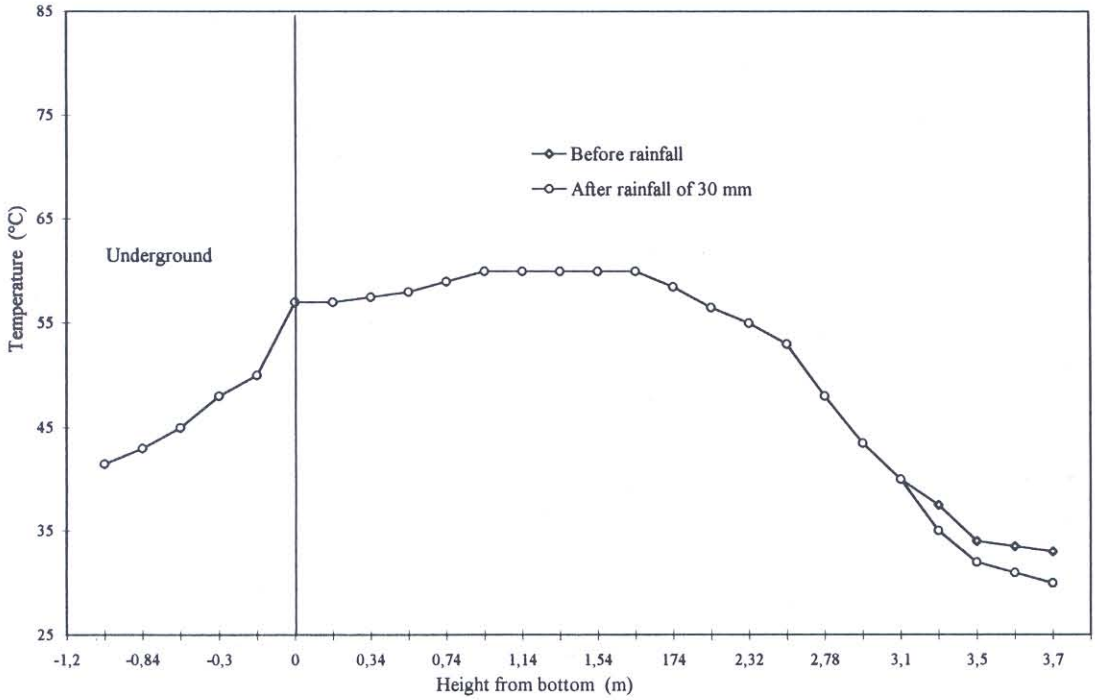

Fig. 11. Effect of rainfall on the temperature profile.

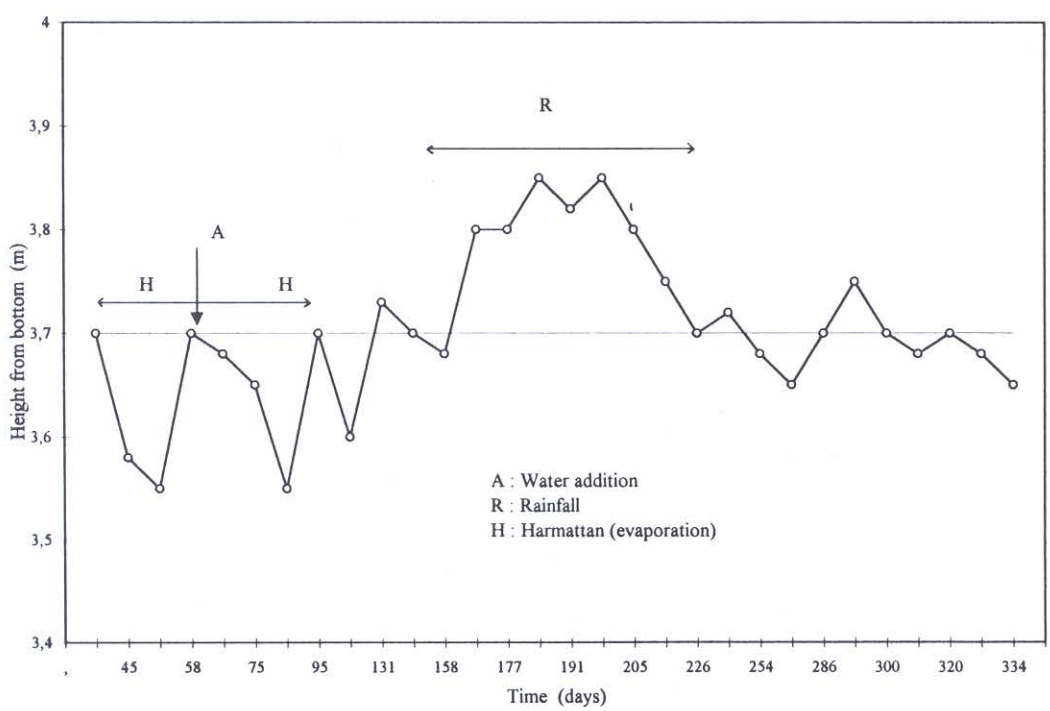

Fig. 12. Water level history in the pond.

6. HEAT EXTRACTION: SPECIFIC APPLICATION OF GRAIN DRYING

Two submerged copper heat exchangers were performed for heat extraction. One is installed at the interface between the *NCZ* and the *LCZ*, and the sealed heat exchanger at the bottom. The copper heat exchanger was 15 m long coiled tubes with 49 mm outside diameter. Periodically, the heat in the pond has been extracted in order to produce hot air, via an external water/air heat exchanger, for grain drying in metallic silos [18].

The performance of this heat exchanger was good. The maximum heat extracted in a day was about 194.0 kWh/day output at 70°C to 76°C. This energy represents 21% of the solar energy incident. The rate of decrease of the mass of copper has been appreciated as being a viable solution.

7. CONCLUSION

The operation of the pond at Lomé in west Africa, a sub-equatorial region, has given a lot of experiences in understanding the behavior. The successful construction and operation of the 200 m² solar pond has demonstrated the technical viability of small solar ponds inspite of the disturbance observed during harmattan.

The works show that solar pond is suitable for heating process, particularly, for grains drying in the tropics. The higher temperature suitable for power generation are reported for Israel where magnesium chloride rich brines are charged in the *LCZ*. Further works should be undertaken including charging the present pond with magnesium chloride rich brines and studying its behavior. And finally, economic analysis would be carried out in order to draw out the economic viability of the pond in the region.

8. ACKNOWLEDGMENTS

Research described in this paper was supported by USAID. The authors wish to thank Dr. Clarence Kooi, and Dr. John Hull for their interest in this work. Their technical and scientific assistance are gratefully appreciated.

9. NOMENCLATURE

A_C	=	area of the solar pond (m)
C_s	=	humid heat capacity of air (kJ/kg°C)
H_0	=	global radiation on a horizontal surface (W/m²)
P_a	=	partial pressure of water vapor in the ambient air (mm Hg)
P_e	=	perimeter of the pond (m)
P_t	=	atmospheric pressure (mm Hg)
P_S	=	partial pressure of water vapor
K	=	thermal conductivity of water (W/m°C)
K_g	=	thermal conductivity of ground (W/m°C)
L_g	=	distance from the bottom of the pond to the ground water table (m)
L_T	=	latent heat of evaporation of water (kJ/kg)
LCZ	=	Lower Convective Zone

UCZ	=	Upper Convective Zone
NCZ	=	Non-Convective Zone
N	=	cloud cover
n	=	sunshine duration (hours/day)
T	=	temperature at any distance x in the pond (°C)
T_a	=	ambient temperature (°C)
T_b	=	bottom convective zone temperature (°C)
T_g	=	ground water temperature (°C)
T_s	=	surface zone temperature (°C)
T_{SKY}	=	sky temperature (°C)
ΔS	=	salinity difference across the gradient zone (%)
ΔT	=	temperature difference across the gradient zone (°C)
Δx	=	optimum gradient thickness (m)
x	=	vertical co-ordinate of the pond (height from the top) (m)
V_a	=	wind velocity (m/s)
α	=	transmittance-absorptance product for solar pond
ε	=	surface albedo
ε_o	=	emissivity of water (%)
σ	=	Stephan-Boletzmann constant (W/m^2K^4)
ϕ	=	relative humidity (%)
η	=	thermal efficiency of the pond (%)

10. REFERENCES

1. Stan Hightower and Bronicki, L. 1987. Installation and operation of the first 100 kW solar pond power plant in the United States. In *Proceedings of the International Progress in Solar Ponds*, Mexico.
2. Tabor, H. Z., and Doron, B. 1987. The Beith Ha'arava 5 MW(e) solar pond power plant (SPPP). Progress Report. In *Proceedings of the International Progress in Solar Ponds*, Mexico.
3. Gninginvi, M., et al. 1986. Solar drying problem in Togo. In *Proceedings of Solar Drying in Africa*, Dakar.
4. Banna, M., and Gninginvi, M. 1998. Estimation of monthly average hourly and daily global irradiation in Togo. *RERIC International Energy Journal* 20(1): 21-37.
5. Joshi, V.; Kishore V.V N.; and Rao, K. S. 1983. A digital simulation of non-convecting solar pond for Indian conditions. In *Proceedings of the International Symposium Workshop on Renewable Energy Sources*, Lahore, Pakistan.
6. Perry, R.H., and Chilton, C.H. (Eds.) 1973. *Chemical Engineers Hand Book. 5th Edtionn*, New York: MacGraw-Hill.
7. McAdams, W.H. 1954. *Heat Transmission. 3rd Edition.* New York: McGraw-Hill.
8. Calingaert, G., and Davis, D.S. 1925. *Ind. Eng. Chem.* 17 1287.
9. Buchberg, H., and Roulet, J. R. 1968. Simulation and optimization of solar collection and storage for house heating. *Solar Energy* 12: 31.
10. Kishore, V.V. N., and Joshi, V. 1984. A practical collection efficiency equation for non-convecting solar ponds. *Solar Energy* 33(5): 391-395.
11. Kooi, C. F. 1979. The steady-state salt gradient solar pond. *Solar Energy* 23: 37-45.
12. Hawlader, M.N.A., and Brinkworth, B. J. 1982. An analysis of the non-convecting solar pond. *Solar Energy* 27: 195.

13. Fynn, R. Peter, and Short, Ted H. 1983. Solar Ponds - A Basic Manual. *Special Circular 106, Ohio Agricultural Research and Development Centre Wooster, Ohio 44691*. Ohio: The Ohio State University.
14. Golding, P., and Nielsen, E. 1987. Brine clarity in solar ponds. Progress Report. In *Proceedings of the International Progress in Solar Ponds*, Mexico.
15. Akbarzadeh, A., and Ahmadi, G. 1981. On the development of the salt concentration profile in a solar pond. *Solar Energy* 6: 369-382.
16. Akbarzadeh, A., and MacDonald, R.W.G. 1982. Introduction of a passive method for salt replenishment in the operation of solar ponds. *Solar Energy* 29: 71-76.
17. Guha, A. 1986. Analysis of Heat Transfer in Solar Ponds. M.E. Dissertation, I.I.Sc. Bangolore.
18. Banna, M., et al. 1995. Bassin solaire à gradient de salinité en Afrique de l'ouest application à la conservation du maïs grains en silo metallique sous atmosphère controllée, *Journal of Engineering for International Development* 2(2): 35-45.